Chapter 6

# Mesoporous Titania: Synthesis, Properties and Comparison with Non-Porous Titania

Barbara Bonelli, Serena Esposito and
Francesca S. Freyria

Additional information is available at the end of the chapter

http://dx.doi.org/10.5772/intechopen.68884

**Abstract**

Some relevant physico-chemical and photocatalytic properties of ordered mesoporous $TiO_2$ as obtained by template-assisted synthesis methods are reported. After a review of the crucial aspects related to different synthesis procedures reported by the literature, the focus is pointed on the (often) superior physico-chemical properties of ordered mesoporous $TiO_2$ with respect to (commercial) bulk $TiO_2$. Those are essentially higher specific surface area and ordered mesoporosity; possibility to control the formation of different crystalline phases by varying the synthesis conditions and possibility to obtain films, nanoparticles with different morphologies and/or materials with hierarchical porosity. Although mesoporous $TiO_2$ is extensively studied for many applications in the fields of photocatalysis, energy and biomedicine, this chapter focuses on the use of mesoporous $TiO_2$ in environmental photocatalysis, by putting in evidence how the physico-chemical properties of the material may affect its photocatalytic behaviour and how mesoporous $TiO_2$ behaves in comparison with commercial $TiO_2$ samples.

**Keywords:** template-assisted synthesis, ordered mesoporosity, $TiO_2$, anatase, photocatalysis, doping

## 1. Introduction

$TiO_2$ is one of the most studied metal oxides: this is mainly due to its intrinsic properties, i.e. occurrence of different polymorphs and amorphous phases, low toxicity to humans, relatively low cost, good chemical and thermal stability and good electronic and optical properties [1]. Such characteristics make $TiO_2$ the oxide of choice for application in (photo)catalysis,

adsorption/separation processes, sensing, energy storage/conversion and biotechnology/biomedicine [1].

Although several commercial products are available on the market, the intrinsic properties of $TiO_2$ may be enhanced in the presence of porous samples that can be obtained by different synthesis procedures [2–9].

Besides increasing the specific surface, porosity facilitates some physico-chemical phenomena like adsorption and diffusion of chemical species, especially in the presence of mesopores (Ø = 2.0–50 nm). Conversely, micropores (Ø ≤ 2.0 nm) may have a detrimental effect on the diffusion of larger moieties.

For instance, mesoporous $TiO_2$ (M-$TiO_2$) was found to be highly active in several photocatalytic processes, since mesopores promote the diffusion of chemical species, either reactants or products [5, 6], and simultaneously enhance M-$TiO_2$ photocatalytic activity by facilitating access to the reactive sites at the photocatalyst surface. Moreover, the possibility to synthesise nanoparticles (NPs) allows obtaining a material that is highly dispersible in solution: consequently, M-$TiO_2$ is not only considered for environmental photocatalytic processes (usually carried out in aqueous phase) but is attracting increasing attention also for applications in biomedicine [7], due to the possibility of controlling NP morphology and size during the synthesis.

Moreover, highly organised films of M-$TiO_2$ may be obtained by evaporation-induced self-assembly (EISA) process [8, 10, 11] in the presence of diblock and triblock copolymers [12–14]. The availability of both EISA process and Pluronic amphiphilic triblock copolymers allowed overcoming the main issue related to the synthesis of M-$TiO_2$, i.e. the high reactivity of Ti precursors, which are usually unstable when exposed to water or even to moisture [15].

Discovered and developed in the 1990s, the first type of ordered mesoporous oxide ever obtained was $SiO_2$, likely due to the high pliability of the Si–O–Si bond, which is a peculiarity of silicon [16, 17]. The synthesis methods leading to the production of ordered mesoporous $SiO_2$-based materials have developed much faster [18] with respect to other mesoporous oxides [19]. Reasons for that have been (i) the lack of suitable metal precursors for sol-gel synthesis and (ii) their lower stability with respect to Si-precursors. Nonetheless, the low thermal stability of some mesoporous oxides may induce formation of undesired crystalline phases and/or grain growth. Such processes are likely at the high temperatures reached during calcination, the process often adopted to remove organic moieties deriving from the template and/or hydrolysis of the (metal alkoxide) precursor [20].

It is possible to obtain M-$TiO_2$ materials with either disordered or ordered mesoporosity. Disordered mesostructures are obtained by template-free methods, whereas the use of a structure-directing agent and/or a template is necessary to obtain ordered mesostructures. Historically, the first attempts to obtain M-$TiO_2$ led to materials characterised by a disordered porosity, which were mainly studied for photocatalytic applications [5]. Ordered mesoporous frameworks are supposed to improve the photocatalytic performance of $TiO_2$, since an ordered porous structure favours diffusion of both reactants and products. The latter class of materials is therefore more interesting for photocatalytic applications in environmental

remediation and is addressed in this chapter. Other types of ordered $TiO_2$ structures, i.e. hollow fibres, nanotubes (not addressed here), are instead obtained by other methods like electrodeposition, electrospinning [21], etc.

Concerning the use of templates, both soft-template methods and hard-template methods are available [2]. The former imply the use of surfactants that form micelles (direct or inverse), whereas hard-template methods imply the use of preformed mesoporous solids like $SiO_2$ or carbon, as well as (natural and/or synthetic) polymers (**Figure 1**).

The physico-chemical properties of the final product depend on several factors, like the chosen Ti precursor, which affects the hydrolysis and condensation reactions occurring during formation of the mesoporous network, and the calcination temperature. Calcination, usually necessary to remove the organic moieties, deriving by both the surfactants used in soft-template methods and the hydrolysis of Ti alkoxides used as Ti precursors, markedly affects the type of $TiO_2$ polymorph formed as well as the size of crystalline grains.

The physico-chemical properties of the final material are very important since they ultimately affect the performance of M-$TiO_2$ in the target application and may be responsible of a better (or worst) performance with respect to commercial products. Among the latter ones, so far, Degussa P25 is the most used and studied commercial $TiO_2$: due to its remarkable photocatalytic performance, it is used as benchmark material in most of the literature works.

Far from having the purpose of reviewing in detail the procedures for the preparation of ordered M-$TiO_2$, only some crucial aspects of the most acknowledged synthesis methods will be addressed in this chapter. Afterwards, the chapter will show some correlations between the peculiar physico-chemical properties of M-$TiO_2$ and its performance in environmental photocatalysis, although the properties of M-$TiO_2$-based systems are attracting considerable attention also for other applications, including $H_2$ production, fabrication of electrodes in Li-ion batteries, dye-sensitised solar cells and biomedicine [22].

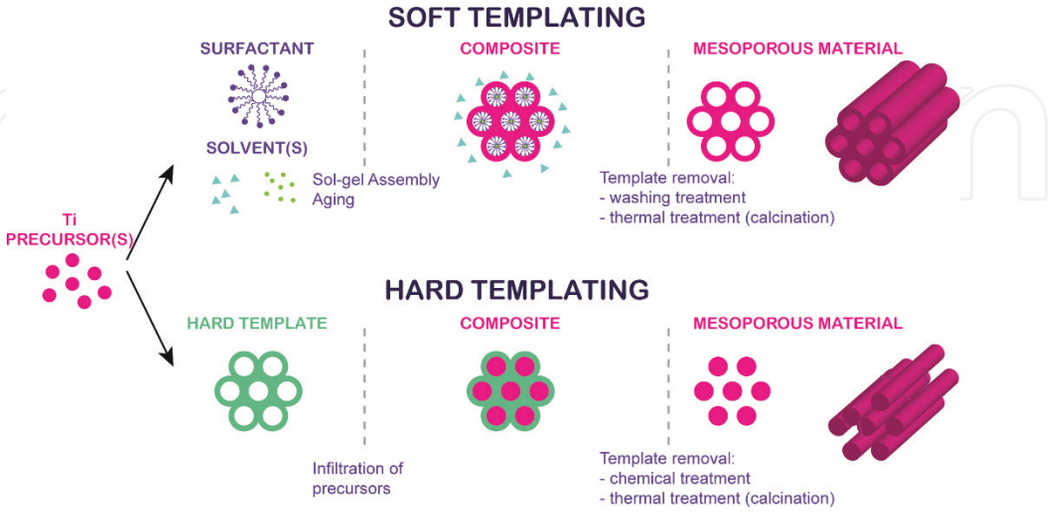


**Figure 1.** Simplified scheme of the steps leading to the production of ordered M-$TiO_2$ by means of template-assisted syntheses.

## 2. Template-based methods for the synthesis of ordered mesoporous titania: main features and critical issues

### 2.1. Hard-template methods: nanocasting

Nanocasting (**Figure 1**, lower part) consists of using preformed (natural or synthetic) mesoporous solids to synthesise porous materials of different compositions: such method has been extensively applied to produce porous carbons, metal oxides and metal sulphides as negative replicas of preformed hard templates [23, 24].

Usually, nanocasting envisages three fundamental steps: (i) the precursor is infiltrated within the mesoporous channels of a porous solid (i.e. preformed mesoporous $SiO_2$ or carbon); (ii) the precursor reacts forming a composite of the negative replica and the hard template and (iii) the hard template is removed (either chemically or thermally).

As a result, a negative replica is obtained of the hard template, which in the case of M-$TiO_2$ is mostly mesoporous $SiO_2$ (e.g. SBA-15, SBA-16, MCM-41, MCM-48, KIT-6, FDU-12), mesoporous carbon (e.g. CMK-1, CMK-3), porous $Al_2O_3$ or polystyrene spheres [5].

Nanocasting allows obtaining M-$TiO_2$ characterised by crystallinity and thermal stability, because it overcomes the problem of thermal collapse of the $TiO_2$ framework, which may occur during phase transition. Some problems, however, may arise during the synthesis: for instance, if the precursor infiltration is performed in aqueous phase, some undesired precipitation and crystallisation of $TiO_2$ in solution may lead to an incomplete filling of the hard-template pores, ultimately blocking the channels and avoiding any further precursor infiltration [15].

In order to avoid such undesired phenomenon, some parameters like precursor/template ratio, calcination temperature and immersion time have to be strictly controlled [25].

A careful evaluation of the weight ratio between the Ti alkoxide and the solid template [25] is crucial, as a too high amount of precursor would lead to formation of bulky material outside the hard-template pores, with consequent loss of surface area and poor precursor infiltration [25].

Conversely, some positive confinement effects due to the hard template in contact with $TiO_2$ allow obtaining anatase M-$TiO_2$ at temperatures that are unusual for bulk $TiO_2$, for instance, with mesoporous silica KIT-6 as hard template, anatase (instead of rutile) M-$TiO_2$ formed by calcination at 750°C [25]. Such result is particularly sound since anatase, though characterised by a larger band gap than rutile ($E_g \cong 3.2$ eV and 3.0 eV for anatase and rutile, respectively), has a large surface area that is very useful for (photo)catalytic applications.

As for the soft-template routes discussed in the following paragraph, the choice of Ti precursor is the main issue. While metal nitrates and chlorides are successfully employed [26] for producing replicas of other metal oxides, Ti nitrates and chlorides are mostly unstable in water (or even when exposed to moisture).

Such problem has been successfully overcome by Yue et al. [27]: they prepared M-$TiO_2$-negative replicas of both SBA-15 and KIT-6 mesoporous silica by pre-hydrolysing the Ti

precursor (either Ti isopropoxide ($Ti[OCH(CH_3)_2]_4$) or tetrabutyl titanate ($Ti[OC_4H_9]_4$) and dissolving it in $HNO_3$. The so-obtained acidic solution of Ti nitrate complexes was used for the infiltration step. Another interesting result was the formation of rutile M-$TiO_2$ at calcination temperatures as low as 100°C, ascribed to either the confinement effect [27] of KIT-6 mesoporous channels or the ability of nitrate ions to stabilise the rutile phase within the $SiO_2$ walls. Indeed, when other Ti precursors are employed (like chloride, sulphate and isopropoxide), anatase M-$TiO_2$ preferentially forms and transition to rutile M-$TiO_2$ is not observed at temperatures as high as 600°C [28].

Nanocasting is feasible also by using naturally occurring hard templates: a fascinating work reports on a nanocrystalline rutile $TiO_2$ obtained by using the chitin scales present on the wings of a *Morpho* butterfly, which were coated with a uniform oxide film by adopting a computer-controlled surface sol-gel process [29]. In addition, the calcination process was a crucial step: when the composite was fired at 450°C, mostly anatase $TiO_2$ formed, whereas firing at 900°C mainly led to rutile, though some anatase was still present in the final product [29].

Hierarchical structures of $TiO_2$ films (**Figure 2**) were obtained by combining PMMA (poly(methyl methacrylate)) microspheres and sol-gel chemistry, in the presence of an amphiphilic diblock copolymer as a structure-directing agent [30]. Poly(dimethylsiloxane)-block-methyl methacrylate poly(ethylene oxide) (PDMS-bMA(PEO)) was used as a structure-directing agent for the preparation of the mesopore structure, whereas PMMA microspheres acted as a template for the micrometre-scale structure (**Figure 3**). Both the hard and the soft templates were then removed either by acetic acid or calcination, leading to a macro/mesoporous network, where the macropores generated by the hard template are supposed to favour mass transport phenomena and improve accessible surface area.

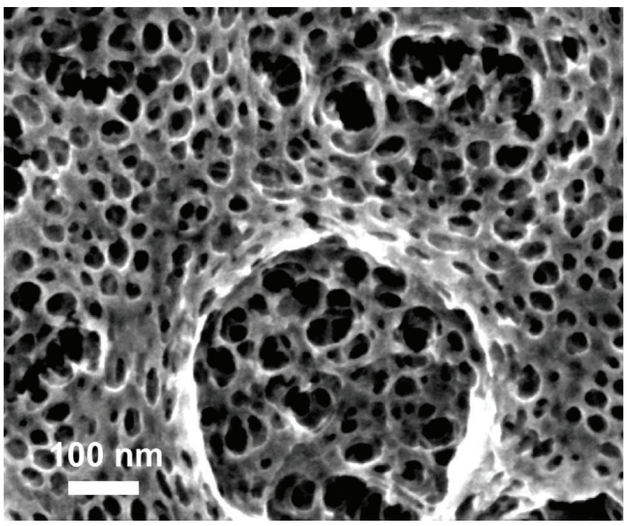


**Figure 2.** SEM image showing the occurrence of macro- and mesopores in a hierarchically structured $TiO_2$ film. (Reprinted with permission from Ref. [30]. Copyright 2009 American Chemical Society).

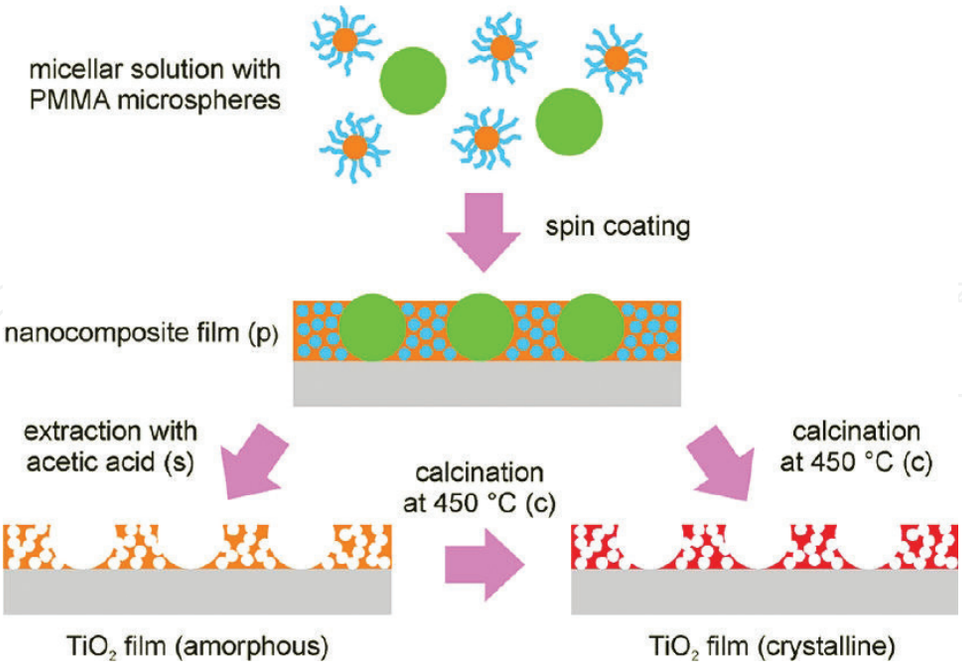


**Figure 3.** Scheme of the procedure adopted to produce hierarchically structured $TiO_2$ films. (Reprinted with permission from Ref. [30]. Copyright 2009 American Chemical Society).

Similarly, a macro/mesoporous $TiO_2$ was obtained by using poly(styrene-co-acrylic acid) colloidal spheres and triblock copolymer Pluronic P123 as macro- and mesoporous structure-directing agents [31], leading to a material with enhanced photoelectrocatalytic activity towards the removal of Rhodamine B.

### 2.2. Soft-template methods

The first report on an aqueous soft-templating route for the synthesis of M-$TiO_2$ dates back to 1995 [32]: soft-template methods employ different types of structure-directing agent, like charged surfactants (either anionic or cationic), neutral surfactants (e.g. alkylamines) and block copolymers [12, 14, 20, 32–38].

The crucial issue is the control of hydrolysis and condensation rates of the Ti precursor during the cooperative assembly between the structure-directing agent and the inorganic phase.

The second major problem is the thermal stability of the so-obtained M-$TiO_2$ framework, especially during the high-temperature calcination step (required to remove the template), since undesired structural collapse and/or crystallisation may occur, leading to the loss of mesoporosity and/or the grain growth.

The Ti precursor stabilisation is particularly difficult when charged surfactants are used: in a pioneering work, Antonelli et al. used acetylacetonate as a ligand to decrease the reactivity of Ti isopropoxide through the formation of Ti acetylacetonate tris(isopropoxide) in the presence of an alkyl phosphate surfactant [32]. The proposed method showed, however, some limits: on the one side, it was not possible to completely remove phosphorous, likely due to the strong

interaction between surfactant and M-$TiO_2$ framework; on the other side, the method was unsuccessful when another charged surfactant (either anionic or cationic) was used.

In a subsequent work, Antonelli obtained a worm-like M-$TiO_2$ by using an amine as template [39]: the material was characterised by short-range order and relatively low thermal stability, as well as high specific surface area (≅700 $m^2$ $g^{-1}$) and the possibility to tune pore dimensions by changing the length of the amine carbon chain (12–18 C atoms). At variance with the alkyl phosphate surfactant used in Ref. [32], where it was not possible to remove phosphorous completely by calcination, when an amine molecules is used, weaker H-bonding interaction occurs between the template and Ti oligomers, finally stabilising the latter species. The main drawback of this method was the longer ageing time required in order to obtain a stable material.

Other attempts with an amine as soft template were made, for instance, with hexadecylamine [40]: the basic molecule seemed to positively affect both hydrolysis and condensation of the Ti precursor, allowing an effective cooperative assembly between the organic and inorganic phase.

However, an effective development of M-$TiO_2$ was reached only with the advent of block copolymers and EISA method [20, 41]. Block copolymers are non-ionic surfactant (**Figure 4a**) consisting of distinct homopolymer subunits (blocks) linked by covalent bonds like the triblock copolymer known under the commercial name of Pluronic P123 (nominal chemical formula $HO(CH_2CH_2O)_{20}(CH_2CH(CH_3)O)_{70}(CH_2CH_2O)_{20}H$).

Such molecules have a high self-assembly capability and may form different mesostructures, depending on their concentration in an alcohol-rich solution [8, 42, 43]: at concentrations below the CMC (critical micelle concentration), each copolymer behaves as a free molecule. At the CMC, copolymer molecules tend to form spherical micelles, with the hydrophobic part in contact with the alcoholic solution and the hydrophilic part shielded within the micelle, in order to minimise the free energy. At concentration above the CMC, coalescence of spherical micelles into cylindrical ones occurs. If the copolymer concentration increases, phase separation may occur, with micelles self-assembling in hexagonal, cubic or lamellar mesophases.

Other types of synthesis imply the use of hydrophobic solvents like cyclohexane and diblock copolymers, known under the commercial name of Brij-n (**Figure 4c**): in those cases, inverse micelles form, with a hydrophilic core that acts as a nanoreactor for the polymerisation of $TiO_x$. The surfactant is then removed by extractions/centrifugation/washing, and then a final calcination step brings about the total removal of the organic part as well as M-$TiO_2$ crystallisation [44]. After calcination, M-$TiO_2$ NPs form aggregates with interparticle porosity (**Figure 4c**).

Concerning the morphology of the final material, it is possible to obtain films in a rather simple way, through the so-called EISA method coupled to the sol-gel technique [20, 43] in ethanol/water mixtures (**Figure 2**). An acid (i.e. HCl) is added to control the sol-gel chemistry of the Ti precursor, which forms Ti hydroxides and/or oligomers. The sol is then deposited on a solid substrate, and solvent evaporation is induced by regulating the relative humidity (RH).

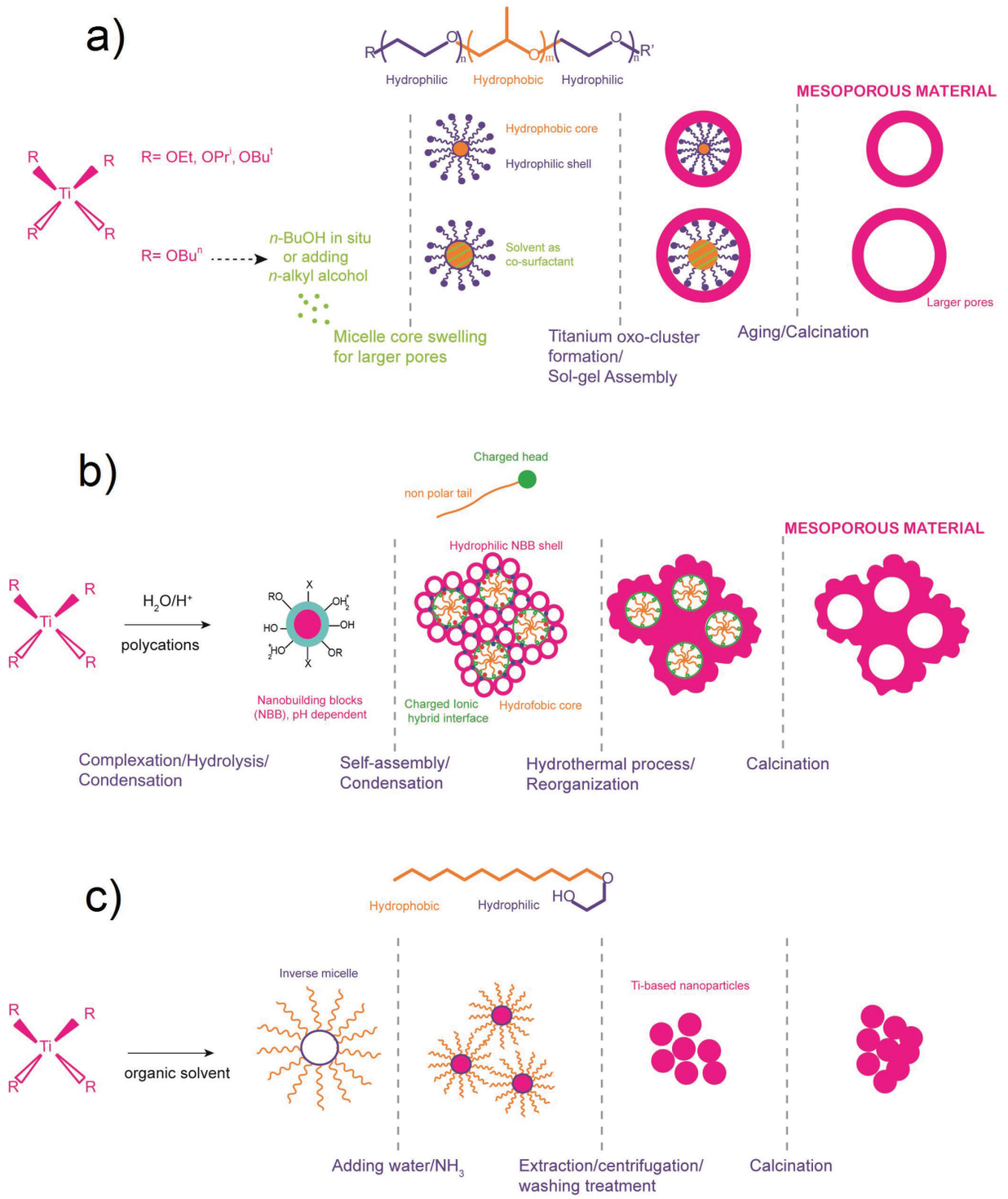


**Figure 4.** Schemes of three synthesis routes that are possible by using as soft template: (a) a triblock copolymer, e.g. Pluronic P123. The optional addition of a swelling agent (like *n*-BuOH) allows tuning mesopore dimension [52]; (b) an ionic surfactant, like cetyltrimethylammonium bromide (CTAB). NBB resulting from partial condensation of the precursor may have a charged surface due to pH-dependent protonation of ≡Ti–OH to ≡Ti–$OH_2^+$ and are stabilised by the negative charge of the anion [50, 51]; and (c) diblock copolymer, such as Brij-n, which forms inverse micelles in cyclohexane [44].

As the solvent evaporates, the concentration of both Ti species and the copolymer increases, and, simultaneously, the assembly of the inorganic and the organic phases is favoured. Induced evaporation also helps the removal of HCl (and other volatile species), improving the long-range order of the obtained film. Indeed, in a previous work where $TiCl_4$ was used as Ti precursor, the molecules of HCl likely induced some hydrolysis in the oxide framework, and rather disordered films were obtained [41].

The order of the final M-$TiO_2$ films obtained by the EISA method (**Figure 5**) depends on the amount of $H_2O$, HCl and RH and crystallisation process, as extensively discussed by Crepaldi et al. [20]. In particular, RH results to be a key parameter during the self-assembly step, as it both affects hydrolysis/condensation of Ti species and polarity of the PEO chain [20]. Moreover, RH was found to affect the order, thickness and transparency of the obtained film.

To further control the hydrolysis and condensation of the Ti precursor during the assembly process, addition of ligands like acetic acid [45] and acetylacetonate [46] usually leads to more ordered and/or more stable materials.

In the EISA method, the initial solution is prepared by dissolving anhydrous $TiCl_4$ into an alcohol-rich solution where the block copolymer has been pre-dissolved. The occurring reaction is

$$TiCl_4 + x\text{EtOH} + y\,E_2\,O \;\rightarrow\; TiCl_{4-x-y}(OEt)_x(OH)_y + (x-y)\text{HCl} \qquad (1)$$

Concerning the Ti precursor, as $TiCl_4$ leads to the formation of HCl through reaction (1) with consequent pH lowering and disordering of the obtained solid [30], stabilised alkoxides are used either as such or mixed with $TiCl_4$ itself [47, 48].

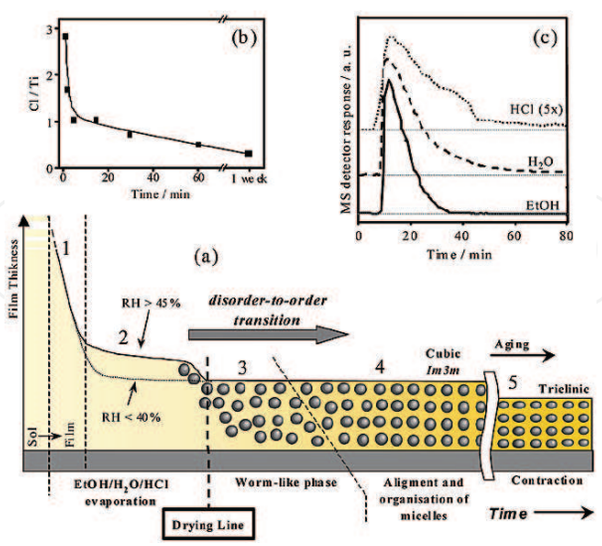


**Figure 5.** Scheme of the steps leading to the formation of M-$TiO_2$ by means of the EISA method. (Adapted from Ref. [20]. Copyright 2003 American Chemical Society).

Ti alkoxides are more easy to handle with respect to $TiCl_4$, but they need some acid as a stabiliser to control the hydrolysis: besides providing acidic conditions, HCl also forms complexes with the Ti alkoxide. For instance, when $Ti(OEt)_4$ is used, the following reaction occurs:

$$\mathrm{Ti(OEt)_4} + (4 - x - y)\mathrm{HCl} + y\,\mathrm{H_2O} \rightarrow \mathrm{TiCl_{4-x-y}(OEt)_x(OH)_y} + (4 - x)\mathrm{EtOH} \quad (2)$$

Starting from different precursors, the same (partially hydrolysed) species $TiCl_{4-x-y}(OEt)_x(OH)_y$ form in the initial sol [49]. Such species are low-molecular-weight oligomers that, being resistant to hydrolysis, act as nanobuilding blocks (NBB) and cooperate with the hydrophilic portion of the copolymer micelles (for instance, by forming H-bonding with the PEO segment in the Pluronic surfactants).

Concerning NBB, their surface is pH-dependent, due to the protonation of ≡Ti—OH groups to ≡Ti—$OH_2^+$, and in the presence of ionic surfactants, they can be stabilised by the charge of ions present in the solution [50, 51], as depicted in **Figure 4b**, where the ionic template may be hexadecyltrimethylammonium bromide (CTAB). Formation of the hybrid composite depends on the CTAB/Ti ratio and pH of the solution [50, 51]. After self-assembly and condensation, NBB are likely located between the micelle and the inorganic framework: the subsequent hydrothermal treatment can promote the condensation of such NBB, finally leading to a robust inorganic mesostructure.

In order to obtain larger mesopores, it is possible to use a swelling agent, like, for instance, an *n*-alkyl alcohol (*n*BuOH), which solubilises the hydrophobic/hydrophilic interface of the micelle, thereby causing it to swell (**Figure 4a**) [52]. The degree of swelling is proportional to the amount of alcohol, which not only acts as a swelling agent but, being likely located at the hydrophilic/hydrophobic interface, also stabilises the liquid crystal phase and determines its curvature at the interface with the inorganic mesostructure [52].

Calcination is the most effective process for the organic template removal, but it is also a crucial step, since the mesoporous network may collapse at high temperature, with consequent loss of specific surface area. Nonetheless, the thermal treatment also induces crystallisation of the initially amorphous material: the degree of crystallinity is of paramount importance for applications like photocatalysis; therefore, the temperature and time of the calcination have to be carefully controlled. A high degree of crystallinity is desirable, as it implies less surface defects, and therefore a better photocatalytic performance, as defects may act as recombination centres, lowering the photocatalyst performance. An opposite concomitant effect is the grain growth, favoured at high temperatures [5].

In order to obtain thermally stable materials, with suitable grain size and few surface defects, different post-synthesis thermal treatments have been proposed in the literature. For instance, it is possible to obtain cubic M-$TiO_2$ with anatase phase stable up to 400°C obtained after 4 h calcination at 400°C (heating rate 1°C/min) [53]. This material was considered as a promising one for photocatalytic (and optoelectronic) applications, whereas the hexagonal M-$TiO_2$ was not stable above 250°C.

M-$TiO_2$ thin films stable up to 600°C [54] due to the presence of rather thick walls (9.0–13 nm), where synthesised by using Pluronic F127 (a triblock polymer with chemical composition:

$PEO_{106}PPO_{70}PEO_{106}$, EO = ethylene oxide, PO = propylene oxide) as the structure-directing agent and tetrabutyl titanate as the precursor, in the presence of acetylacetonate [54]. According to the authors, the use of Pluronic F127 as the structure-directing agent favoured the formation of thick $TiO_2$ framework.

Another work reported [55] on the preparation of a M-$TiO_2$ stable up to 650°C obtained by a carbonisation step of the organic template with $H_2SO_4$ followed by thermal treatment at 350°C in inert atmosphere ($N_2$). Such process led to the formation of tubular C deposits that acted as stabilisers of $TiO_2$ during the calcination at a high temperature carried out through different steps (first at 550 and 650°C in $N_2$ and then at 450°C in air to burn out the carbon). The final material was a highly ordered 2D hexagonal mesostructure, with a crystalline framework arising by the connection of anatase nanocrystals. The ordered M-$TiO_2$ obtained had high surface area (~193 $cm^2\ g^{-1}$), large pore volume (~0.23 $cm^3\ g^{-1}$) high thermal stability (~650°C) and uniform mesopore size (4.6–5.1 nm).

Stabilisation of M-$TiO_2$ with larger mesopores (Ø > 5.0 nm) is still a challenge and requires some post-treatment methods. For instance, a modified EISA approach envisages the use of ethylene diamine molecules [56], which effectively protect the M-$TiO_2$ primary particles from collapsing finally delaying the phase transition of anatase to rutile. According to this method [56], a M-$TiO_2$ with large pore size (10 nm), high surface area (122 $m^2\ g^{-1}$) and thermal stability up to 700 °C was obtained.

Other factors controlling the phenomena occurring during the synthesis of M-$TiO_2$ materials (not be addressed here) have been extensively reviewed in the literature [2, 5, 8].

## 3. Photocatalytic applications of M-$TiO_2$

Photocatalytic processes involving $TiO_2$ are among the most common advanced oxidation processes (AOPs) proposed for the degradation of several inorganic and organic environmental pollutants [57, 58]. Ordered mesoporous structures are highly desirable for photocatalytic applications, since sufficiently large mesopores facilitate diffusion of reactants/products and high specific surface area improves adsorption, especially when bulky organic moieties are implied, like in wastewater and groundwater remediation.

### 3.1. Photocatalytic properties of pure M-$TiO_2$

Positive effects ascribable to the occurrence of an ordered mesoporous structure were observed in the photocatalytic degradation of methylene blue (MB), a dye commonly used in this type of studies as a model molecule of recalcitrant organic pollutants that are resistant to biodegradation and for which a photocatalytic treatment is necessary.

For instance, a M-$TiO_2$ occurring as pure anatase phase showed good photocatalytic activity towards MB removal [59]. The best photocatalyst was a hexagonal M-$TiO_2$ obtained by sol-gel synthesis using CTAB as template and Ti isopropoxide as precursor. The material obtained

through a 6-days sol-gel synthesis showed mesopores with 6.86 nm diameter and a specific surface area of 284 $m^2 g^{-1}$. Longer synthesis time led to a decrease of both values and to the simultaneous disappearance of the hexagonal mesophase. The sample showed indeed a sizeable MB degradation with respect to Degussa P25, especially after M-$TiO_2$ was recycled and contacted with a fresh MB solution. Such superior photocatalytic behaviour was assigned to both higher surface area and higher anatase content of M-$TiO_2$ with respect to Degussa P25 [60].

Satisfactory results concerning the photobleaching of MB were obtained with a M-$TiO_2$ using SBA-15 silica as hard template, the activity of the sample being again ascribed to a compromise between its high surface area and the percentage of anatase. The former parameter was likely responsible for a very efficient dye adsorption at the surface of M-$TiO_2$, the latter likely reduced the electron/hole ($e^-/h^+$) recombination, which is slow in crystalline and defect-free materials [28].

A M-$TiO_2$ photocatalyst obtained through the EISA method by employing ethylene diamine as a stabiliser showed better photocatalytic activity than Degussa P25 towards the degradation of 2,4-dichlorophenol, a toxic chlorinated compound produced by environmental transformations of some chlorinated herbicides and/or antimicrobial agents [56]. Several M-$TiO_2$ were studied and compared to Degussa P25: the most efficient degradation was obtained in the presence of a M-$TiO_2$ calcined at 700°C, whereas the performance of M-$TiO_2$ calcined at higher temperatures decreased. Moreover, the performance of the M-$TiO_2$ photocatalyst resulted stable after recycling. The photocatalytic behaviour of the studied materials was explained not only on the basis of a higher surface area (122 $m^2 g^{-1}$) with respect to Degussa P25 (ca. 50 $m^2 g^{-1}$): according to the authors, a trade-off exists between the occurrence of pure anatase phase and a well-ordered mesoporous structure facilitating diffusion of reactants/products. At higher calcination temperatures, i.e. 900°C rutile M-$TiO_2$, formed, with a lower activity. Nonetheless, the sample calcined at 800°C, though occurring as pure anatase, showed both a partial collapse of mesoporous walls and the formation of larger particles, leading to a worst photocatalytic performance.

A performance comparable with Degussa P25 towards the degradation of dimethyl phthalate (a persistent antiparasite) was obtained with M-$TiO_2$ prepared by using Pluronic P123 in weak acidic solution of acetic acid [60]. Similarly to what mentioned before, both the high surface area and the crystallinity of the anatase phase contribute to the catalytic activity of the sample.

As a whole, although different experimental conditions are adopted during photocatalytic tests carried out in different laboratories, the occurrence of pure anatase M-$TiO_2$ usually favours better photocatalytic performances under UV radiation. However, this is just a general rule, but several exceptions are observed. For instance, another M-$TiO_2$ obtained by soft-template route under high-intensity ultrasound irradiation showed better photocatalytic performance than P25 in the UV-assisted degradation of *n*-pentane in air (**Figure 6**). The studied M-$TiO_2$ was not pure anatase, but a bi-crystalline material, containing ca. 20% brookite and 80% anatase, the formation of brookite being ascribed to the ultrasound treatment adopted during the synthesis [61]. The M-$TiO_2$ samples after calcination were

characterised by high surface area (112–128 $m^2\ g^{-1}$) and the occurrence of both anatase and brookite phase (**Figure 7**).

The band gap of the as-prepared M-$TiO_2$ materials (SM-1 and SM-2) was estimated through Tauc's plot since the band gap of brookite should be ca. 0.16 eV higher than that of anatase and could contribute to a more efficient UV light absorption, indicating that brookite could be a more powerful photocatalyst. According to the authors, composite materials of brookite and anatase can also suppress $e^-/h^+$ recombination, similarly to what widely accepted for Degussa P25 (i.e. that its high photocatalytic activity is partially due the coexistence of 80% anatase and 20% rutile, which can inhibit the recombination of excited $e^-/h^+$ [62]).

Other authors found a positive effect of the incorporation of Degussa P25 particles in M-$TiO_2$ thin films [63]: the films were tested in the photocatalytic degradation of Acid Black Dye, used as a model molecule of textile water pollutants. As expected, Degussa P25 incorporation led to a decrease of surface area in the composite with respect to M-$TiO_2$ films: however, a 5.0 wt.% Degussa P25 content led to an increase in the dye degradation efficiency. The positive role of Degussa P25 was ascribed both to an increase of the M-$TiO_2$ film thickness and to the presence of rutile in Degussa P25 leading to a band-gap change in the composite.

Another major use of $TiO_2$ is in disinfection processes: to this respect, wormhole like anatase M-$TiO_2$ was studied for the photocatalytic disinfection of *Escherichia coli*, showing better performances with respect to Degussa P25 [64].

### 3.2. Photocatalytic properties of metals doped M-$TiO_2$

Processes like doping and modification of $TiO_2$ are usually required in order to decrease the recombination rate of $e^-/h^+$ pairs and to extend the absorption range towards the Vis [65]. The latter effect is particularly important in the perspective of exploiting solar light, especially for photocatalytic processes of environmental remediation that have to be carried out under solar illumination in view of actual large-scale applications [66, 67].

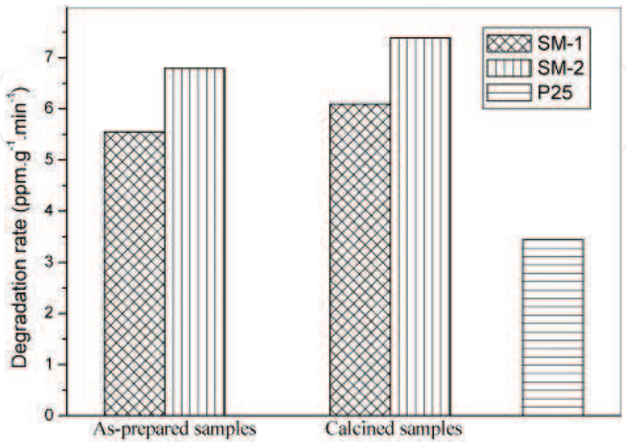


**Figure 6.** Rates of UV-assisted degradation of *n*-pentane as catalysed by two M-$TiO_2$ (SM-1 and SM-2) obtained under high-intensity ultrasound irradiation are compared to the rate obtained by using Degussa P25 (after Ref. [61]). (Copyright 2002 American Chemical Society).

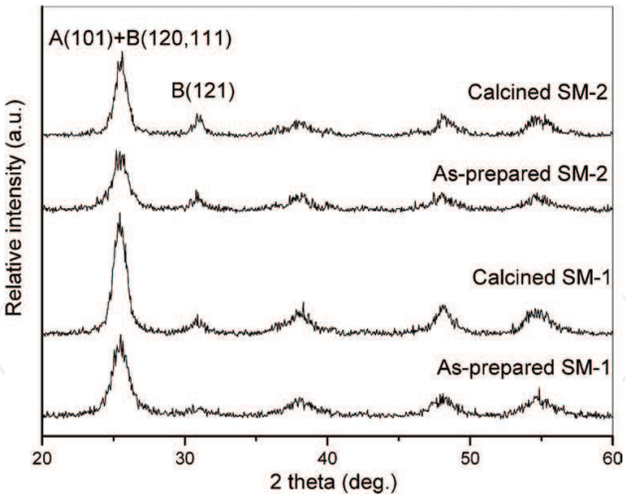


**Figure 7.** XRD patterns of the as-prepared and calcined M-$TiO_2$ (SM-1 and SM-2) obtained under high-intensity ultrasound irradiation: A denotes anatase; B denotes brookite [61]. (Copyright 2002 American Chemical Society).

As expected, the photocatalytic activity of M-$TiO_2$ is significantly improved after doping with metals and non-metals. Besides doping, other methods are used to modify the photocatalytic properties of M-$TiO_2$, like, for instance, the synthesis of solid solutions or of different $TiO_2$ composites with noble metals, other metal oxides and quantum dots (not addressed here) [5].

Fe is one of the most used metals for doping: on the one side, it extends the absorption of $TiO_2$ in the Vis range; on the other side, Fe species present at the surface may give rise to Fenton-like reactions [68], finally enhancing the reactivity merely due to the photocatalytic process (vide infra).

A Fe-doped M-$TiO_2$ was used to obtain composites with hollow glass microbeads: the latter were able to prevent aggregation of M-$TiO_2$ NPs [69]. As expected, Fe doping induced a red shift of the absorption band. Consequently, an effective photodegradation of methyl orange (a model molecule of azo dyes) in aqueous solution was achieved under visible light ($\lambda > 420$ nm) irradiation, revealing the potential applicability of such nanocomposites in some industry fields, like water purification.

A Fe-doped M-$TiO_2$ (with 2.5 wt.% Fe content) obtained by direct synthesis resulted very active towards the catalytic degradation of Acid Orange 7 (a model molecule of azo dyes) not only under UV irradiation but also in dark conditions in the presence of $H_2O_2$ [70, 71]. The dark process was studied in detail, showing that since not all Fe species entered the M-$TiO_2$ framework, surface $Fe^{3+}$ species were very active in Fenton-like reaction. Though limited Fe leaching was observed, the Fe-doped M-$TiO_2$ was still active after reactivation in air. Preliminary results concerning the test reaction under UV-Vis illumination provided further support to this picture. The authors used the same synthesis protocol for V-doping, but in that case, it was not possible to obtain an actual doping, since all the V species resulted present at the surface of the catalyst. In any case, the studied M-$TiO_2$ materials showed remarkable high specific surface area (150–120 $m^2\ g^{-1}$) and pure anatase NPs.

The effect of other metals used for doping is more complex. For instance, when Ce was used to produce doped thin films of M-$TiO_2$ [72], Ce species were likely located at the surfaces/grain boundaries of M-$TiO_2$ crystallites, due to the larger size of $Ce^{3+}/Ce^{4+}$ ions with respect to $Ti^{4+}$ ions. High levels of Ce doping, instead, adversely affected the crystallisation of nanocrystalline anatase since Ce–O–Ti bonds at the grain boundaries inhibited crystallite growth.

The optimal amount of Ce doping corresponded to a ratio Ce/Ti = 0.3 mol%: the corresponding Ce-doped M-$TiO_2$ showed a remarkable photocatalytic activity towards the degradation of MB (**Figure 8**). The enhanced photocatalytic activity of the Ce-doped M-$TiO_2$ with Ce/Ti = 0.3 mol% was assigned to enhanced electron transport and oxygen storage capabilities in the presence of Ce, along with the highly nanocrystalline nature of the $TiO_2$ framework.

### 3.3. Photocatalytic properties of non-metal doped M-$TiO_2$

Doping with non-metals (mainly C, N, S, F and $I_2$ [5]) is also supposed to extend $TiO_2$ absorption towards the Vis range. The mechanisms responsible of such phenomenon are complex and usually related to either the narrowing of $TiO_2$ band gap or the creation of intermediate steps within the band gap [66], due to the non-metal atoms substituting oxygen atoms in the framework.

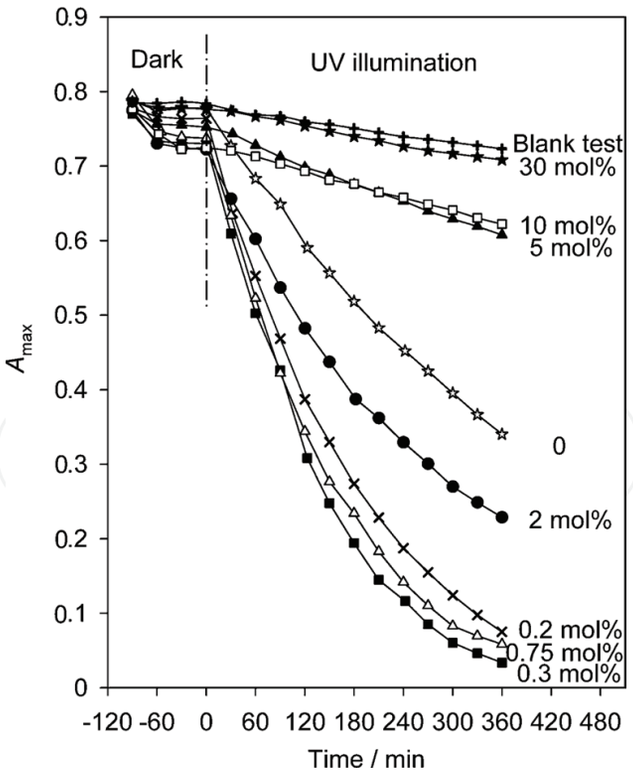


**Figure 8.** Changes in absorption maximum of MB as a function of exposure time during photocatalytic tests carried out with Ce-doped M-$TiO_2$ thin films. The best results are obtained with a Ce/Ti = 0.3 mol% composition (after Ref. [72]). (Copyright 2009 American Chemical Society).

N is one of the most used non-metals, as doping may be carried out rather simply by thermally treating M-$TiO_2$ under $NH_{3(g)}$ flow or by heating a M-$TiO_2$ produced in solutions containing a N source ($NH_3$, urea, etc.).

The ultimate effect of N of the light absorption capacity of the sample is however complex and may be due to different processes:

(i) Band-gap narrowing due to $N_{2p}$ states close in energy to $O_{2p}$ states

(ii) Formation of impurity energy levels above the valence band

(iii) Partial doping in oxygen vacancies

All this notwithstanding, literature reports on N-doped M-$TiO_2$ materials with improved photocatalytic properties. For instance, by a template-free combustion method, a wormhole M-$TiO_2$ was obtained, where N doping was due to the presence of urea during combustion [73]. The so-obtained N-doped M-$TiO_2$ occurred as nanocrystalline anatase phase, showing high surface area (234 $m^2\ g^{-1}$) and type-IV H3-mesoporosity.

Two photocatalytic reactions were studied, namely, Rhodamine B degradation and *p*-anisyl alcohol oxidation to *p*-anisaldehyde in aqueous solution under direct sunlight. Notwithstanding the high band gap (3.24 eV) of the N-doped sample, the good activity was assigned to a better utilisation of holes due to the low-charge diffusion barrier associated with wormhole mesoporosity along with the occurrence of crystalline NPs, finally confirming the importance of having an ordered mesoporous photocatalyst.

N-doped anatase M-$TiO_2$ was prepared via soft-template route by using CTAB as template and by treating in $NH_3$ (70%)/$N_2$ atmosphere the calcined samples. The material was characterised by small crystallite size, large surface area (420–126 $m^2\ g^{-1}$ for calcination temperatures in the 400–800°C range), high crystallinity and Vis light response. The N-doped anatase M-$TiO_2$ photocatalysts showed much higher photocatalytic activity than N-doped Degussa P25 for the degradation of phenol under both UV and Vis light irradiation, owing to more oxidising hydroxyl radicals, which were the oxidative species mainly responsible for the degradation of phenol [74]. The authors concluded that the materials might be beneficial to solar-driven applications in the photodegradation of organic pollutants.

However, the effect of doping on the photocatalytic performance is not straightforward, as it has been observed that N-doped $TiO_2$ shows visible light-responsive photocatalytic activity but lower UV light-responsive photocatalytic activity. The visible light photocatalytic activity originates from new N 2*p* levels near the valence band. The oxygen vacancies and the associated $Ti^{3+}$ species act as the recombination centres for the photoinduced $e^-/h^+$, finally reducing photocatalytic activity although contributing to Vis light absorbance [75].

## 4. Conclusions

The production of mesoporous titania by template-assisted methods allows obtaining materials characterised by ordered mesoporous structure, controllable crystallinity, high surface

area and tuneable pore size. Moreover, powder nanoparticles or films may be obtained, as well as hierarchical porosity materials.

From the point of view of photocatalytic applications, the type of crystalline phase and ordered mesopores are crucial factors: the former may be responsible of more efficient UV light absorption and slower electron-hole recombination rate; the latter positively affect diffusion processes and mass transfer phenomena. Nonetheless, the possibility of obtaining high surface area materials, also after calcination, positively affects any kind of heterogeneous catalytic process, besides photocatalytic ones, as mesoporous titania may be an efficient support for other types of catalytically active phases.

Several mesoporous titania materials reported by the literature have remarkable photocatalytic properties and are competitive, at least on a lab scale, with commercial samples. It must be considered, however, that template-assisted syntheses require high-cost reagents and/or energy-intensive steps, like calcination.

However, for applications requiring tailored photocatalysts, the progresses made on the side of synthesis procedures will surely allow the development of promising (photo)catalysts based on mesoporous titania.

## Author details

Barbara Bonelli[1]*, Serena Esposito[2] and Francesca S. Freyria[1,3]

*Address all correspondence to: barbara.bonelli@polito.it

1 Department of Applied Science and Technology, INSTM Turin-Polytechnic Unit, Polytechnic University of Turin, Turin, Italy

2 Department of Civil and Mechanical Engineering, University of Cassino and Southern Lazio, Cassino, Italy

3 Department of Chemistry, Massachusetts Institute of Technology, Cambridge, MA, USA

## References

[1] Chen X, Mao S. Titanium dioxide nanomaterials: Synthesis, properties, modifications and applications. Chemical Reviews 2007;**107**(7):2891-2959. DOI: 10.1021/cr0500535

[2] Li W, Wu Z, Wang J, Elzatahry AA, Zhao D. A perspective on mesoporous $TiO_2$ materials. Chemistry of Materials. 2014;**26**:287-298. DOI: 10.1021/cm4014859

[3] Boettcher SW, Fan J, Tsung C-K, Shi Q, Stucky GD. Harnessing the sol–gel process for the assembly of non-silicate mesostructured oxide materials. Accounts of Chemical Research. 2007;**40**:784-792. DOI: 10.1021/ar6000389

[4] Zhang R, Elzatahry AA, Al-Deyab SS, Zhao D. Mesoporous titania: From synthesis to application. Nano Today. 2012;**7**(4):344-366. DOI: 10.1016/j.nantod.2012.06.012

[5] Zhou W, Fu H. Mesoporous $TiO_2$: Preparation, doping, and as a composite for photocatalysis. ChemCatChem. 2015;**5**:885-894. DOI: 10.1002/cctc.201200519

[6] Ismail AA, Bahnemann DW. Mesoporous titania photocatalysts: Preparation, characterization and reaction mechanisms. Journal of Materials Chemistry. 2011;**21**(32):11686-11707. DOI: 10.1039/C1JM10407A

[7] Vivero-Escoto JL, Chiang YD, Wu KC-W, Yamauchi Y. Recent progress in mesoporous titania materials: Adjusting morphology for innovative applications. Science and Techn ology of Advanced Materials. 2012;**13**:013003. DOI: 10.1088/1468-6996/13/1/013003

[8] Pan JH, Zhao XS, Lee WI . Block copolymer-templated synthesis of highly organized mesoporous $TiO_2$-based films and their photoelectrochemical applications. Chemical Engineering Journal. 2011; **170**(2-3):363-380. DOI: 10.1016/j.cej.2010.11.040

[9] Pan JH, Dou H, Xiong Z, Xu C, Ma J, Zhao XS. Porous photocatalysts for advanced water purifications. Journal of Materials Chemistry. 2010;**20**(22):4521-4528. DOI: 10.1039/B925523K

[10] Brinker CJ, Lu Y, Sellinger A, Fan H. Evaporation-induced self-assembly: Nanostructures made easy. Advanced Materials. 1999;**11**:579-585. DOI: 0935-9648/99/0705-0579

[11] Lu Y, Ganguli R, Drewien CA, Anderson MT, Brinker CJ, Gong W et al. Continuous formation of supported cubic and hexagonal mesoporous films by sol-gel dip-coating. Nature. 1997;**389**:364-368. DOI: 10.1038/38699

[12] Zhao D, Feng Q, Huo Q, Melosh N, Fredrickson GH, Chmelka BF, Stucky GD. Triblock copolymer synthesis of mesoporous silica with periodic 50-300 angstrom pores. Science. 1998;**279**:548-552. DOI: 10.1126/science.279.5350.548

[13] Zhao D, Huo Q, Fen J, Chmelka BF, Stucky GD. Nonionic triblock and star diblock copolymer and oligomeric surfactant syntheses of highly ordered, hydrothermally stable, mesoporous silica structure. Journal of the American Chemical Society. 1998;**120**(24):6024-6036 . DOI: 10.1021/ja974925i

[14] Zhao D, Yang P, Melosh N, Feng J, Chmelka BF, Stuky G. Continuous mesoporous silica films with highly ordered large pore structure. Advanced Materials. 1998;**10**(16):130-1385. DOI: 10.1002/(SICI)1521-4095(199811)10:16<1380::AID-ADMA1380>3.0.CO;2-8

[15] Livage J, Henry M, Snachez C. Sol-gel chemistry of transition metal oxides. Progress in Solid State Chemistry. 1988;**18**:259-341. DOI: 10.1016/0079-6786(88)90005-2

[16] Kresge CT, Leonowicz ME, Roth WJ, Vartuli J, Beck JS. Ordered mesoporous molecular sieves prepared with liquid crystal templates. Nature. 1992;**359**:710-712

[17] Beck JS, Vartuli JC, Roth WJ, Leonowicz ME, Kresge CT, Schmitt KD et al. A new family of mesoporous molecular sieves prepared with liquid crystal templates. Journal of the American Chemical Society. 1992;**114**:10834-10843. DOI: 10.1021/ja00053a020

[18] Wan Y, Zhao D. On the controllable soft-templating approach to mesoporous silicates. Chemical Reviews. 2007;**107**(7):2821-2860. DOI: 10.1021/cr068020s

[19] Kung HH, Ko EI. Preparation of oxide catalysts and catalyst supports—A review of recent advances. Chemical Engineering Journal. 1996;**64**(2):203-214. DOI: 10.1016/S0923-0467(96)03139-9

[20] Crepaldi EL, Soler-Illia GJdAA, Grosso D, Cagnol F, Ribot F, Sanchez C. Controlled formation of highly organized mesoporous titania thin films: From mesostructured hybrids to mesoporous nanoanatase $TiO_2$. Journal of the American Chemical Society. 2003;**125**(32):9770-9786. DOI: 10.1021/ja030070g

[21] Hou H, Shang M, Wang L, Li W, Tang B, Yang W. Efficient photocatalytic activities of $TiO_2$ hollow fibers with mixed phases and mesoporous walls. Scientific Reports. 2015;**5**:15228. DOI: 10.1038/srep15228

[22] Antonio E. H. Machado, Karen A. Borges, Tatiana A. Silva, Lidiaine M. Santos, Mariana F. Borges, Werick A. Machado, Bruno P. Caixeta, Marcela Dias França, Samuel M. Oliveira, Alam G. Trovó and Antonio O.T. Patrocínio (2015). Applications of Mesoporous Ordered Semiconductor Materials — Case Study of $TiO_2$, Solar Radiation Applications, Ms. Segun R. Bello (Ed.), InTech, DOI: 10.5772/59602. Available from: https://www.intechopen.com/books/solar-radiation-applications/applications-of-mesoporous-ordered-semiconductor-materials-case-study-of-tio2

[23] Yang HF, Zhao DY. Synthesis of replica mesostructures by the nanocasting strategy. Journal of Materials Chemistry. 2005;**15**:1217-1231. DOI: 10.1039/B414402C

[24] Lu AH, Schüth F. Nanocasting: A versatile strategy for creating nanostructured porous materials. Advanced Materials. 2006;**18**:1793-1805. DOI: 10.1002/adma.200600148

[25] Zhang Z, Zuo F, Feng P. Hard template synthesis of crystalline mesoporous anatase $TiO_2$ for photocatalytic hydrogen evolution. Journal of Materials Chemistry. 2010;**20**(11):2206-2212. DOI: 10.1039/B921157H

[26] Ren Y, Ma Z, Bruce PG. Ordered mesoporous metal oxides: Synthesis and applications. Chemical Society Reviews. 2012;**41**:4909-4927. DOI: 10.1039/C2CS35086F

[27] Yue W, Xu X, Irvine JT, Attidekou PS, Liu C, He H et al. Mesoporous monocrystalline $TiO_2$ and its solid-state electrochemical properties. Chemistry of Materials. 2009;**21**:2540-2546. DOI: 10.1021/cm900197p

[28] Yue W, Randorn C, Attidekou PS, Liu C, Irvine JTS, Zhou W. Syntheses, Li insertion, and photoactivity of mesoporous crystalline $TiO_2$. Advanced Functional Materials. 2009;**19**:2826-2833. DOI: 10.1002/adfm.200900658

[29] Weatherspoon MR, Cai Y, Srinivasarao M, Sandhage KH. 3D rutile titania-based structures with *Morpho* butterfly wing scale morphologies. Angewandte Chemie, International Edition. 2008;**47**:7921-7923. DOI: 10.1002/anie.20081311

[30] Kaune G, Memesa M, Meier R, Ruderer MA, Diethert A, Roth SV et al. Hierarchically structured titania films prepared by polymer/colloidal templating. ACS Applied Materials and Interfaces. 2009;**1**(12):2862-2869. DOI: 10.1021/am900592u

[31] Sun W, Zhou S, You B, Wu L. Facile fabrication and high photoelectric properties of hierarchically ordered porous $TiO_2$. Chemistry of Materials. 2012;**24**:3800-3810. DOI: 10.1021/cm302464g

[32] Antonelli DM, Ying JY. Synthesis of hexagonally packed mesoporous $TiO_2$ by a modified sol–gel method. Angewandte Chemie International Edition in English. 1995;**34**(18):2014-2017. DOI: 10.1002/anie.199520141

[33] Kluson P, Kacer P, Cajthlam T, Kalaji M. Preparation of titania mesoporous materials using a surfactant mediated sol-gel method. Journal of Materials Chemistry. 2001;**11**:644-651. DOI: 10.1039/b004760k

[34] Zimny K, Roques-Carmes T, Carteret C, Stébé MJ, Blin JL. Synthesis and photoactivity of ordered mesoporous titania with a semicrystalline framework. Journal of Physical Chemistry C. 2012;**116**(11):6585-6594. DOI: 10.1021/jp212428k

[35] Wang D, Choi D, Yang Z, Viswanathan VV, Nie Z, Wang C et al. Synthesis and Li-ion insertion properties of highly crystalline mesoporous rutile $TiO_2$. Chemistry of Materials. 2008;**20**(10):3435-3442. DOI: 10.1021/cm8002589

[36] Yoshitake H, Sugihara T, Tatsumi T. Preparation of wormhole-like mesoporous $TiO_2$ with an extremely large surface area and stabilization of its surface by chemical vapor deposition. Chemistry of Materials. 2002;**14**(3):1023-1029. DOI: 10.1021/cm010539b

[37] Choi H, Antoniou MG, Pelaez M, de La Cruz AA, Shoemaker JA, Dionysiou DD. Mesoporous nitrogen-doped $TiO_2$ for the photocatalytic destruction of the cyanobacterial toxin microcystin-LR under visible light irradiation. Environmental Science and Technology. 2007; **41**(21):7530-7535. DOI: 10.1021/es0709122

[38] Zhao D, Peng T, Lu L, Cai P, Jiang P, Bian Z. Effect of annealing temperature on the photoelectrochemical properties of dye-sensitized solar cells made with mesoporous $TiO_2$ nanoparticles. Journal of Physical Chemistry C. 2008;**112**(22):8486-8494. DOI: 10.1021/jp800127x

[39] Antonelli DM. Synthesis of phosphorus-free mesoporous titania via templating with amine surfactants. Microporous and Mesoporous Materials. 1999;**30**(2-3):315-319. DOI: 10.1016/S1387-1811(99)00042-6

[40] Chen D, Cao L, Huang F, Imperia P, Cheng Y-B, Caruso RA. Synthesis of monodisperse mesoporous titania beads with controllable diameter, high surface areas, and variable pore diameters (14–23 nm). Journal of the American Chemical Society. 2010;**132**(12):4438-4444. DOI: 10.1021/ja100040p

[41] Yang P, Zhao D, Margolese DL, Chmelka BF, Stucky GD. Generalized syntheses of large-pore mesoporous metal oxides with semicrystalline frameworks. Nature. 1998;**396**:152-155. DOI: 10.1038/24132

[42] Bucknall DG Anderson HL. Polymers get organized. Science. 2003;**302**(5652):1904-1905. DOI: 10.1126/science.1091064

[43] Grosso D, Cagnol F, Soler-Illia GJDAA, Crepaldi EL, Amenitisch H, Brunet-Bruneau A et al. Fundamentals of mesostructuring through evaporation-induced self-assembly. Advanced Functional Materials. 2004;**14**(4):309-322. DOI: 10.1002/adfm.200305036

[44] Chandra P, Doke DS, Umbarkar SB, Biradar AV. One-pot synthesis of ultrasmall $MoO_3$ nanoparticles supported on $SiO_2$, $TiO_2$, and $ZrO_2$ nanospheres: An efficient epoxidation catalyst. Journal of Materials Chemistry A. 2014;**2**:19060-19066. DOI: 10.1039/c4ta03754e

[45] Fan J, Boettcher SW, Study GD. Nanoparticle assembly of ordered multicomponent mesostructured metal oxides via a versatile sol-gel process. Chemistry of Materials. 2006;**18**(26):6391-6396. DOI: 10.1021/cm062359d

[46] Zhang J, Deng Y, Gu D, Wang S, She L, Che R et al. Ligand-assisted assembly approach to synthesize large-pore ordered mesoporous titania with thermally stable and crystalline framework. Advanced Energy Materials. 2011;**1**:241-248. DOI: 10.1002/aenm.201000004

[47] Tian B, Yang H, Liu X, Xie S, Yu C, Fan J et al. Fast preparation of highly ordered nonsiliceous mesoporous materials via mixed inorganic precursors. Chemical Communications. 2002;**17**:1824-1825. DOI: 10.1039/B205006D

[48] Tian B, Lu X, Tu B, Yu C, Fan J, Wang L et al. Self-adjusted synthesis of ordered stable mesoporous minerals by acid–base pairs. Nature Materials. 2003;**2**:159-163. DOI: 10.1038/nmat838

[49] Crepaldi EL, Soler-Illia GJDAA, Grosso D, Sanchez C. Nanocrystallized titania and zirconia mesoporous thin films exhibiting enhanced thermal stability. New Journal of Chemistry. 2003;**27**:9-13. DOI: 10.1039/b205497n

[50] Soler-Illia GJdAA, Louis A, Sanchez C. Synthesis and characterization of mesostructured titania-based materials through evaporation-induced self-assembly. Chemistry of Materials. 2002;**14**:750-759. DOI: 10.1021/cm011217a.

[51] Peng T, Zhao D, Dai K, Shi W, Hirao K. Synthesis of titanium dioxide nanoparticles with mesoporous anatase wall and high photocatalytic activity. Journal of Physical Chemistry B. 2005;**109**(11):4947-4952. DOI: 10.1021/jp044771r.

[52] Liu K, Fu H, Shi K, Xiao F, Jing L, Xin B. Preparation of large-pore mesoporous nanocrystalline $TiO_2$ thin films with tailored pore diameters. Journal of Physical Chemistry B. 2005;**109**(40):18719-18722. DOI: 10.1021/jp054546p

[53] Alberius PCA, Frindell KL, Hayward RC, Kramer EJ, Stucky GD, Chmelka, BF. General predictive syntheses of cubic, hexagonal, and lamellar silica and titania mesostructured thin films. Chemistry of Materials. 2002;**14**:3284-3294. DOI: 10.1021/cm011209u

[54] Li H, Wang J, Li H, Yin S, Sato T. High thermal stability thick wall mesoporous titania thin films. Materials Letters. 2009;**63**(18-19):1583-1585. DOI: 10.1016/j.matlet.2009.04.017

[55] Zhang R, To B, Zhao D. Synthesis of highly stable and crystalline mesoporous anatase by using a simple surfactant sulfuric acid carbonization method. Chemistry—A European Journal. 2010;**16**:9977-9981. DOI: 10.1002/chem.201001241

[56] Zhou W, Sun F, Pan K, Tian G, Jiang B, Ren Z et al. Well-ordered large-pore mesoporous anatase $TiO_2$ with Remarkably high thermal stability and improved crystallinity: Preparation, characterization, and photocatalytic performance. Advanced Functional Materials. 2011;**21**(10):1922-1930. DOI: 10.1002/adfm.201002535

[57] Compagnoni M, Ramis G, Freyria FS, Armandi M, Bonelli B, Rossetti I. Photocatalytic processes for the abatement of N-containing pollutants from waste water. Part 1: Inorganic pollutants. Journal of Nanoscience and Nanotechnology. 2017;**17**(6):3632-3653. DOI: 10.1166/jnn.2017.14006

[58] Freyria FS, Armandi M, Compagnoni M, Ramis G, Rossetti I, Bonelli B. Catalytic and photocatalytic processes for the abatement of N-containing pollutants from wastewater. Part 2: Organic pollutants. Journal of Nanoscience and Nanotechnology. 2017;**17**(6):3654-3672. DOI: 10.1166/jnn.2017.14014

[59] Kao L-H, Hsu T-C, Cheng K-K. Novel synthesis of high-surface-area ordered mesoporous $TiO_2$ with anatase framework for photocatalytic applications. Journal of Colloid and Interface Science. 2010;**341**:359-365. DOI: 10.1016/j.jcis.2009.09.058

[60] Liu J, An T, Li G, Bao N, Sheng G, Fu J. Preparation and characterization of highly active mesoporous $TiO_2$ photocatalysts by hydrothermal synthesis under weak acid conditions. Microporous and Mesoporous Materials. 2009;**124**:197-203. DOI: 10.1016/j.micromeso.2009.05.009

[61] Yu JC, Zhang L, Yu J. Direct sonochemical preparation and characterization of highly active mesoporous $TiO_2$ with a bicrystalline framework. Chemistry of Materials. 2002;**14**:4647-4653. DOI: 10.1021/cm0203924

[62] Bickley RI, Gonzalez-Carreno T,Lees JS, Palmisano L, Tilly RJD. A structural investigation of titanium dioxide photocatalysts. Journal of Solid State Chemistry. 1991;**92**: 178-190. DOI: 10.1016/0022-4596(91)90255-G

[63] Sreethawong T, Ngamsinlapasathian S, Yoshikawa S. Positive role of incorporating P25 $TiO_2$ to mesoporous-assembled $TiO_2$ thin films for improving photocatalytic dye degradation efficiency. Journal of Colloid and Interface Science. 2014;**430**:184-192. DOI: 10.1016/j.jcis.2014.05.032

[64] Kim E-Y, Kim,DS, Ahn B-T. Synthesis of mesoporous $TiO_2$ and its application to photocatalytic activation of Methylene Blue and *E. coli*. Bulletin of the Korean Chemical Society. 2009;**30**(1):193-196

[65] Chen X, Shen S, Guo L, Mao SS. Semiconductor-based photocatalytic hydrogen generation. Chemical Reviews. 2010;**110**:6503-6570. DOI: 10.1021/cr1001645

[66] Malato S, Fernández-Ibáñez P, Maldonado MI, Blanco J, Gernjak W. Decontamination and disinfection of water by solar photocatalysis: Recent overview and trends. Catalysis Today. 2009;**147**(1):1-59. DOI: 10.1016/j.cattod.2009.06.018

[67] Chong MN, Jin B, Chow CWK, Saint C. Recent developments in photocatalytic water treatment technology: A review. Water Research. 2010;**44**:2997-3027. DOI: 10.1016/j.watres.2010.02.039

[68] Pignatello JJ, Liu D, Houston P. Evidence for an additional oxidant in the photoassisted fenton reaction. Environmental Science & Technology. 1999;**33**:1832-1839. DOI: 10.1021/es980969b

[69] Cui L, Wang Y, Niu M, Chen G, Cheng Y. Synthesis and visible light photocatalysis of Fe-doped $TiO_2$ mesoporous layers deposited on hollow glass microbeads. Journal of Solid State Chemistry. 2009;**182**(10):2785-2790. DOI: 10.1016/j.jssc.2009.07.045

[70] Piumetti M, Freyria FS, Armandi M, Geobaldo F, Garrone E, Bonelli B. Fe- and V-doped mesoporous titania prepared by direct synthesis: Characterization and role in the oxidation of AO7 by $H_2O_2$ in the dark. Catalysis Today. 2014;**227**:71-79. DOI: 10.1016/j.cattod.2013.11.013

[71] Piumetti M, Freyria FS, Armandi M, Saracco G, Garrone E, Bonelli B. Anti-oxidant/pro-oxidant activity of ascorbic acid: Effect in the degradation of Acid Orange 7 with $H_2O_2$ catalyzed by transition metal ions. Chemistry Today. 2015;**33**(3):40-45.

[72] Zhang Y, Yuwono AH, Wang J, Li J. Enhanced photocatalysis by doping cerium into mesoporous titania thin films. Journal of Physical Chemistry C. 2009;**113**(51):21406-21412. DOI: 10.1021/jp907901k

[73] Sivanarjani K, Gopinath CS. Porosity driven photocatalytic activity of wormhole mesoporous $TiO_2$-xNx in direct sunlight. Journal of Materials Chemistry. 2011;**21**:2639-2647. DOI: 10.1039/C0JM03825C

[74] Tian G, Chen Y, Pan K, Wang D, Zhou W, Ren Z et al. Efficient visible light-induced degradation of phenol on N-doped anatase $TiO_2$ with large surface area and high crystallinity. Applied Surface Science. 2010;**256**(12):3740-3745. DOI: 10.1016/j.apsusc.2010.01.016

[75] Wang J, Tafen DN, Lewis JP, Hong Z, Manivavnnan A et al. Origin of photocatalytic activity of nitrogen-doped $TiO_2$ nanobelts. Journal of the American Chemical Society. 2009;**131**(34):12290-12297. DOI: 10.1021/ja903781h

IntechOpen